Design of spatially-varying orthotropic infill structures using multiscale topology optimization and explicit de-homogenization

Authors: Jaewook Lee[a,*], Chiyoung Kwon[a], Jeonghoon Yoo[b], Seungjae Min[c], Tsuyoshi Nomura[d], and Ercan M. Dede[e]

[a] Gwangju Institute of Science and Technology (GIST), Gwangju, South Korea

[b] Yonsei University, Seoul, South Korea

[c] Hanyang University, Seoul, South Korea

[d] Toyota Central R & D Labs, Aichi, Japan

[e] Toyota Research Institute of North American, Ann Arbor, MI, USA

[*] Presenting author

TOP Webinar 11

Apr. 29, 2021.

Gwangju Institute of Science and Technology

Part I

Introduction

Background

Coated orthotropic infill (shell porous-infill) structures

- ✓ **Biomimetic structure** - Exists in nature such as animal bones, and plant stems
- ✓ **Advantages** of shell porous-infill structure: Superior energy absorption, high strength-weight ratio, Robustness to load variation and material deficiency
- ✓ **Uninform infill** versus **Graded** (spatially-varying thickness and orientation) **infill**

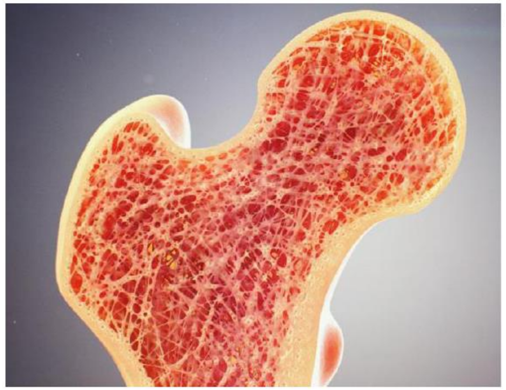

Human femur bone[*]

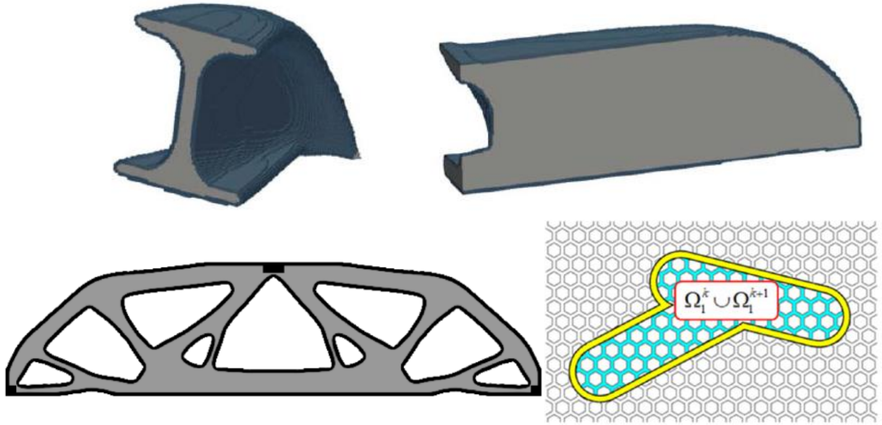

Uniform infill[*,**,***]

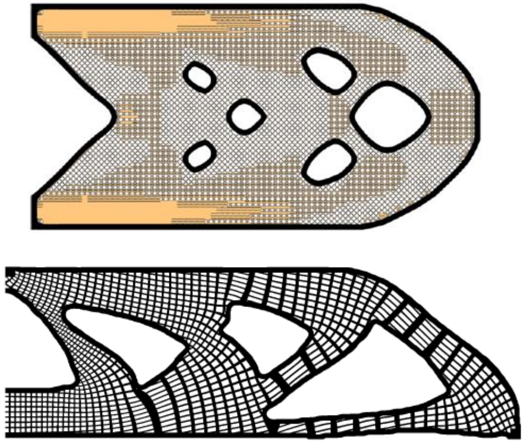

Graded infill[****,*****]

[*] Y. Luo, Q. Li, and S. Liu, Topology optimization of shell-infill structures using an erosion-based interface identification method, CMAME, 2019

[**] A. Clausen, E. Andreassen, O. Sigmund, Topology optimization of 3D shell structures with porous infill, Acta Mech Sin, 2017

[***] V. Hoang, P. Tran, N. Nguyeb, K. Hackl, H. Nguyen-Xuan, Adaptive concurrent topology optimization of coated structures…, CAD, 2020

[****] S. Chu, L. Gao, M. Xiao, Y. Zhang, Multiscale topology optimization for coated structures with multifarious-microstructural infill, SMO, 2020

[*****] J.P. Groen, J. Wu, O. Sigmund, Homogenization-based stiffness optimization and projection of 2D coated structures with orthotropic infill, CMAME, 2019

Gwangju Institute of Science and Technology

Background

Topology Optimization for Shell-infill Structures

➡ Requires two design schemes for (1) Coated macrostructure, (2) Graded porous Infill

(1) Coated macrostructure design

- ✓ Various approaches have been proposed based on smoothed (filtered) density field.
- ✓ Coating region is identified as material interface between void and solid region.

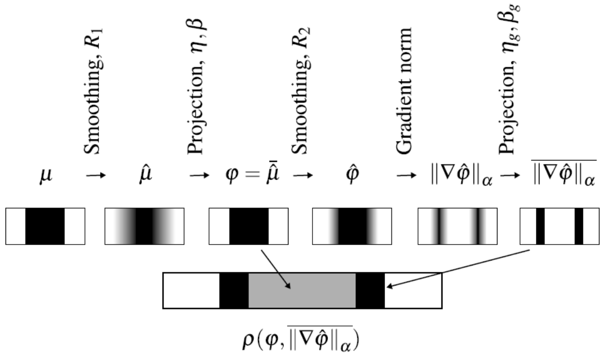

Single smoothing and projection approach*

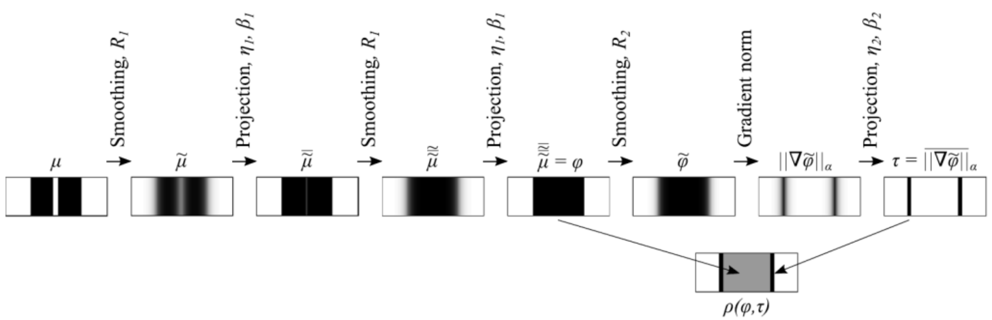

Double smoothing and projection approach**

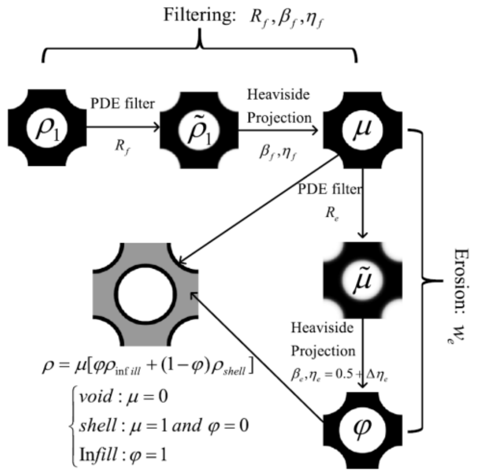

Erosion-based approach***

* A. Clausen, N. Aage, O. Sigmund, Topology optimization of coated structures and material interface problems, CMAME, 2015

** J.P. Groen, J. Wu, O. Sigmund, Homogenization-based stiffness optimization and projection of 2D coated structures with orthotropic infill, CMAME, 2019

*** Y. Luo, Q. Li, and S. Liu, Topology optimization of shell-infill structures using an erosion-based interface identification method, CMAME, 2019

Background

Topology Optimization for Shell-infill Structures

(2) Graded porous infill design: Three approaches

A. Local volume constraint in single macroscale[*,**]

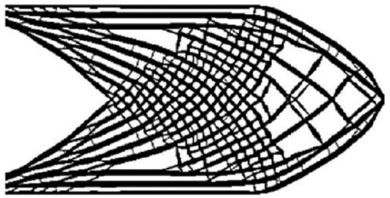

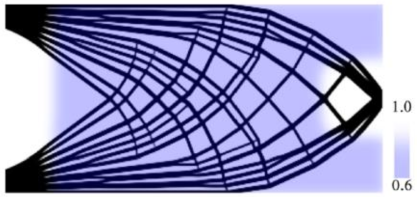

- ✓ Straightforward single-scale approach
- ✓ High computational cost for large-sized macrostructure with small-sized infill

B. Concurrent topology optimization[***,****]

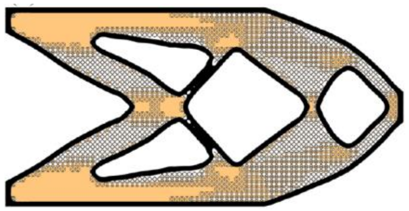

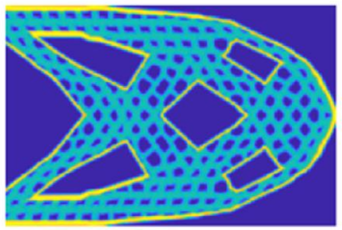

- ✓ Abundant flexibility in infill design
- ✓ High computational cost
- ✓ Require to work on connecting infill microstructures

C. Homogenization-based multiscale approach[****,*****]

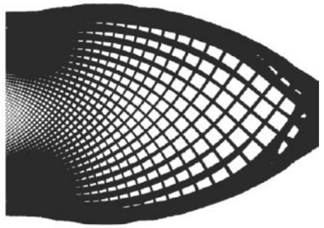

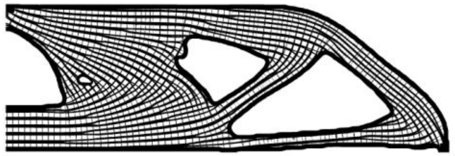

- ✓ Computationally efficient
- ✓ Post-processing is required to restore infill microstructures

[*] J. Wu, N. Aage, R. Westermann, O. Sigumnd, Infill optimization for additive manufacturing, IEEE VCG, 2018
[**] M. Schmidt, C.B.W. Pedersen, C. Gout, On structural optimization using graded porosity control, SMO, 2019
[***] S. Chu, L. Gao, M. Xiao, Y. Zhang, Multiscale topology optimization for coated structures with multifarious-microstructural infill, SMO, 2020
[****] V. Hoang, P. Tran, N. Nguyeb, K. Hackl, H. Nguyen-Xuan, Adaptive concurrent topology optimization of coated structures..., CAD, 2020
[*****] P. Geoffroy-Donders, G. Allaire, G. Michailidis, O. Pantz, Coupled optimization of macroscopic structures and lattice infill, IJNME, 2020
[******] J.P. Groen, J. Wu, O. Sigmund, Homogenization-based stiffness optimization and projection of 2D coated structures with orthotropic infill, CMAME, 2019

Research Objective

Proposed topology optimization of shell-infill structure for additive manufacturing

- ✓ Five sequential design procedures based on homogenization-based multiscale approach
- ✓ Design of coated structure with spatially-varying (functionally graded) infill microstructures
- ✓ Limited in two-dimensional single-load problem

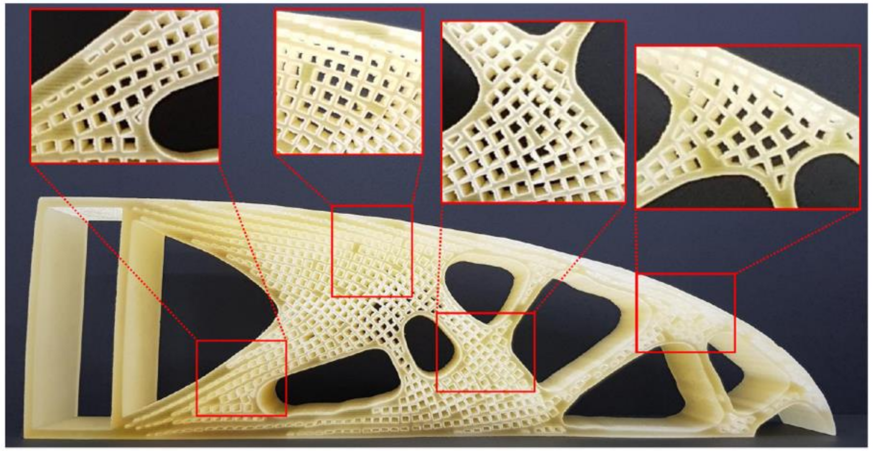

additive manufactured design result

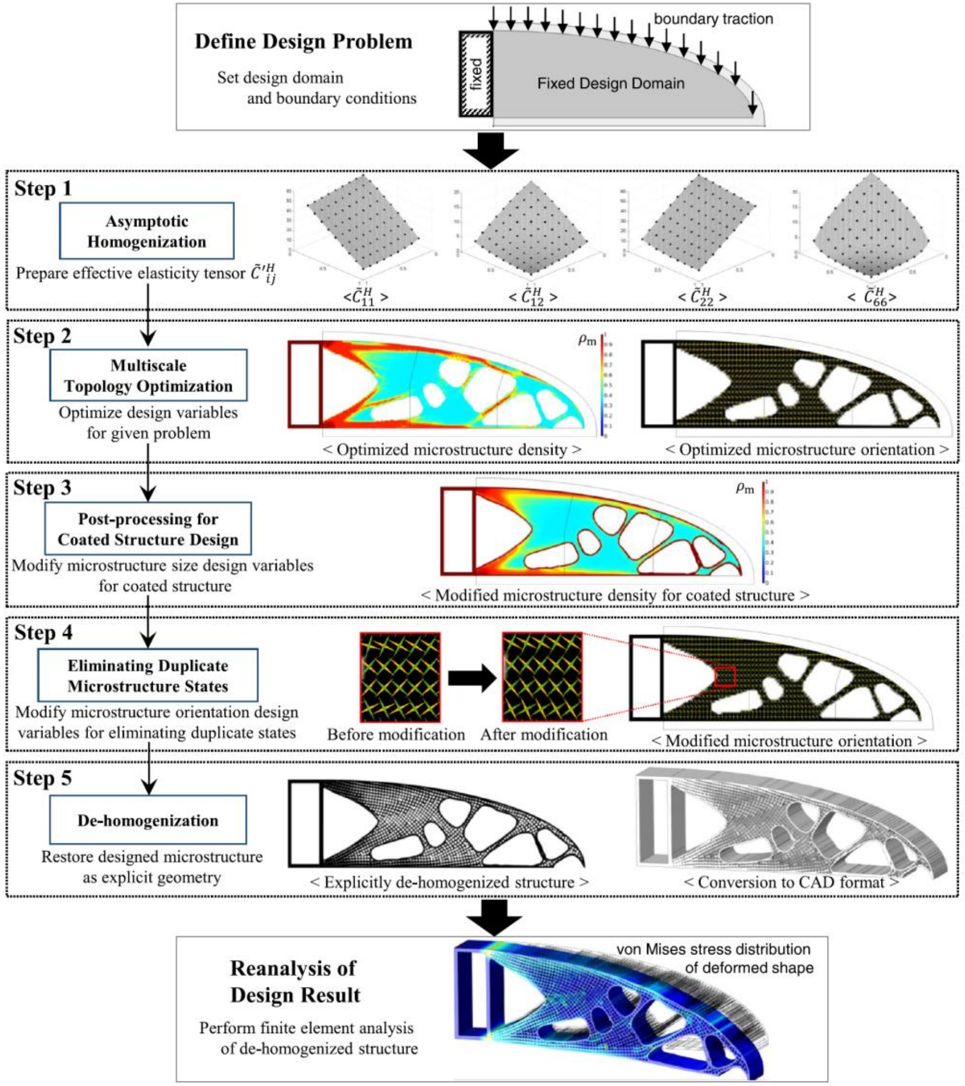

Design procedures

Key Ideas

A. Design of coated macrostructure

- ✓ Straightforward sequential post-processing approach based on filtered density
- ✓ Suitable for graded infill structure
- ✓ Not suitable if coating structure is critical

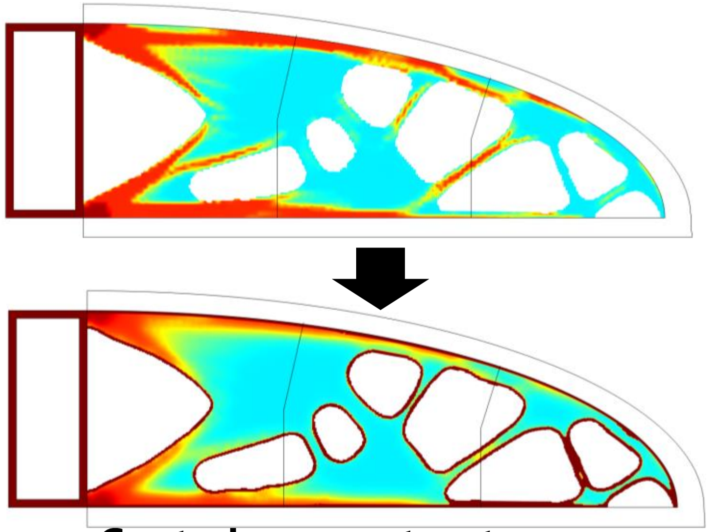

Coated macrostructure

B. Design of infill microstructures

- ✓ Orthotropic infill microstructure is restored as explicit geometry using rotated rectangular
- ✓ Easy to generate mesh of design result for re-analysis
- ✓ Suitable for additive manufacturing

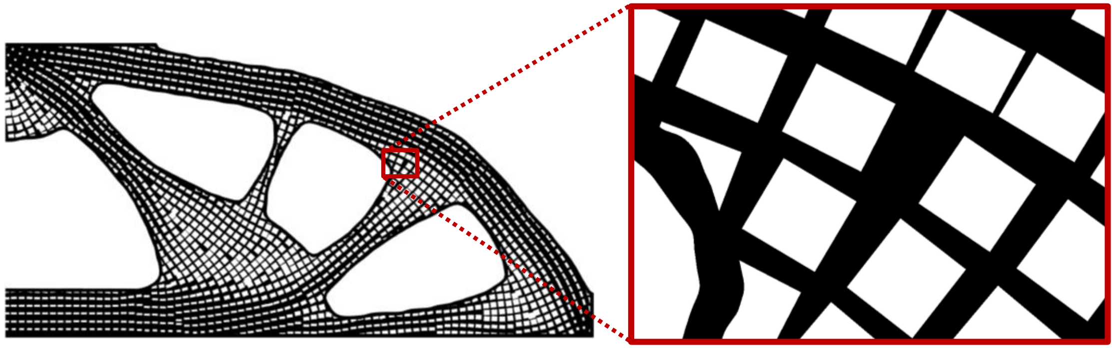

Infill structure using rotated rectangular

Part 2

Topology Optimization Formulation

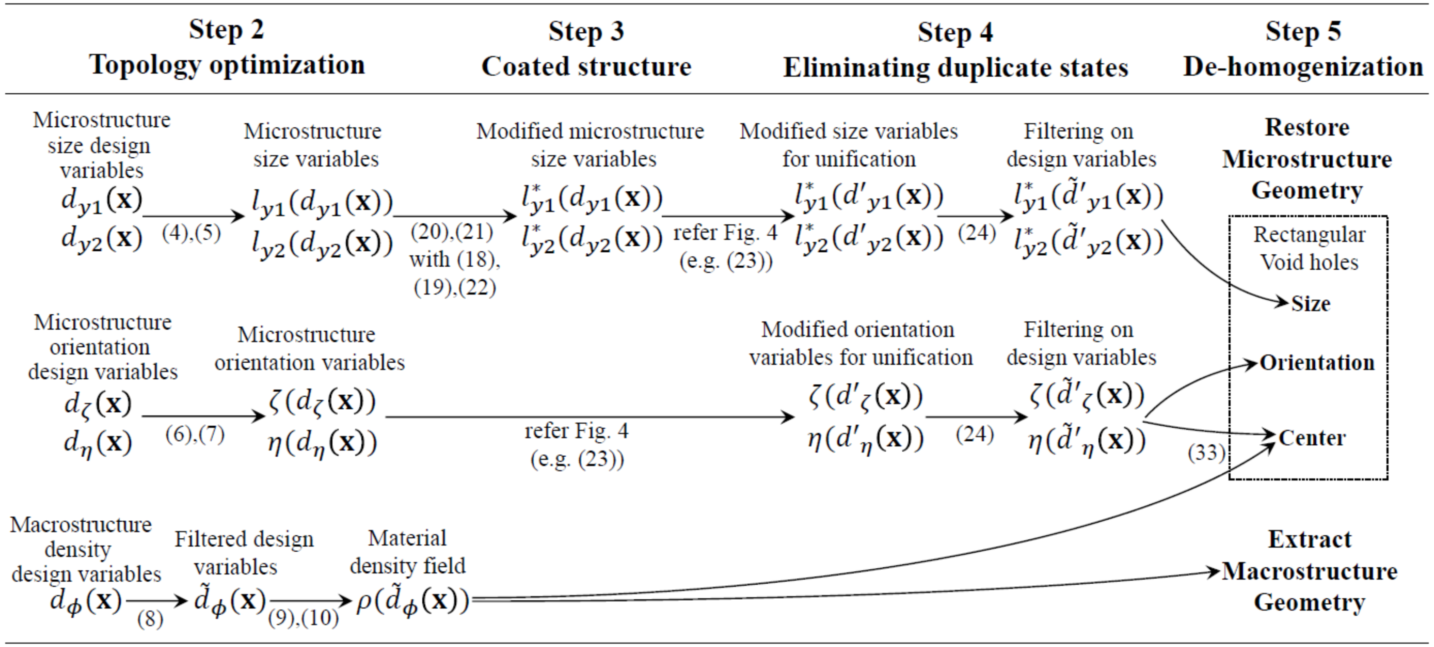

Gwangju Institute of Science and Technology

A. Design of coated macrostructure

Sequential post-processing step after designing macrostructure and infill

- ✓ Simultaneous design of coated macrostructure and infill densities may cause 0-1 convergence problem
- ✓ Ambiguity between macrostructure density $\boldsymbol{\rho}$, and microstructure hole size fields $\mathbf{l}_{\mathbf{y1}}$ and $\mathbf{l}_{\mathbf{y2}}$
- ✓ Coating region may cause sudden change in material property

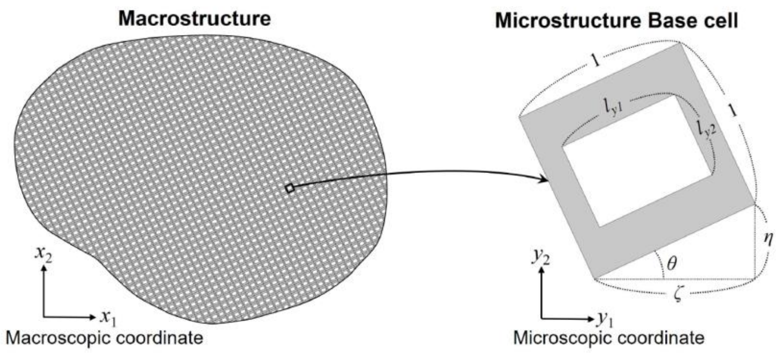

$$-R_\phi^2 \nabla^2 \tilde{d}_\phi(\mathbf{x}) + \tilde{d}_\phi(\mathbf{x}) = d_\phi(\mathbf{x})$$

$$\rho(\mathbf{x}) = H_r(\tilde{d}_\phi(\mathbf{x}))$$

$$l_{y1}(\mathbf{x}) = \frac{l_{upper} - l_{lower}}{2}(d_{y1}(\mathbf{x}) + 1) + l_{lower}$$

$$l_{y2}(\mathbf{x}) = \frac{l_{upper} - l_{lower}}{2}(d_{y2}(\mathbf{x}) + 1) + l_{lower}$$

$$C_{ij}^{\rho}(\mathbf{x}) = C^{void} + \rho(d_\phi)^p(\tilde{C'}_{ij}^H(d_{y1}, d_{y2}, d_\zeta, d_\eta) - C^{void})$$

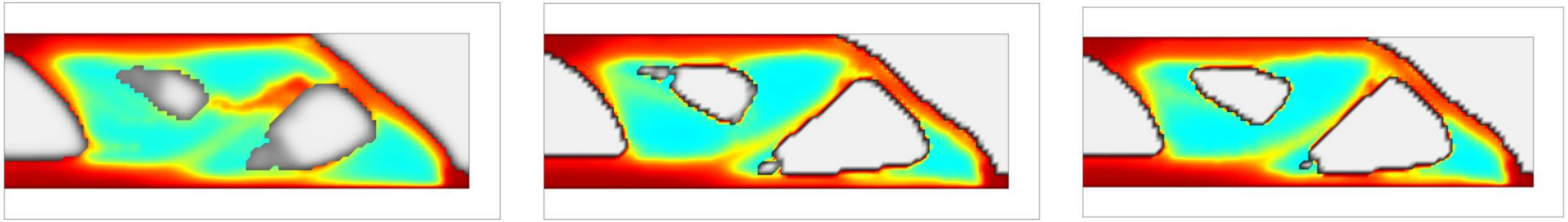

Problem in 0-1convergence of macrostructure density

A. Design of coated macrostructure

Post-processing step after designing macrostructure and infill

- ✓ To avoid this convergence problem, sequential approach is proposed for coated structure design
- ✓ After designing macrostructure without coating and infill density, infill density is set to 1 (i.e. hole sizes l_{y1} and l_{y2} is forced to be 0) at the interface of macrostructure density

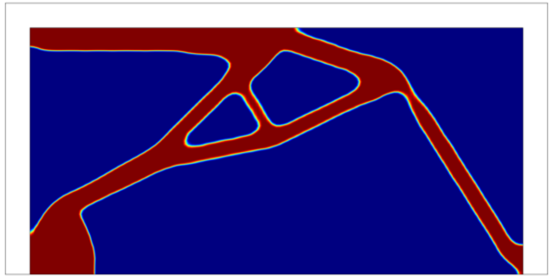

Macrostructure density ρ

$$-R_\rho^2 \nabla^2 \tilde{\rho}(\mathbf{x}) + \tilde{\rho}(\mathbf{x}) = \begin{cases} \rho(\mathbf{x}) & \text{in } D \\ 0 & \text{in } D_{ext} \end{cases}$$

$$\rho_{bnd}(\mathbf{x}) = \begin{cases} 1 & \text{if} \quad 0.1 < \tilde{\rho}(\mathbf{x}) < 0.9 \\ 0 & \text{otherwise} \end{cases}$$

$$w_{bnd}(\mathbf{x}) = 1 - c_{bnd}\rho_{bnd}(\mathbf{x})$$

$$l_{y1}^*(\mathbf{x}) = w_{bnd}(\mathbf{x}) \left[\frac{l_{upper} - l_{lower}}{2} (d_{y1}(\mathbf{x}) + 1) + l_{lower} \right]$$

$$l_{y2}^*(\mathbf{x}) = w_{bnd}(\mathbf{x}) \left[\frac{l_{upper} - l_{lower}}{2} (d_{y2}(\mathbf{x}) + 1) + l_{lower} \right]$$

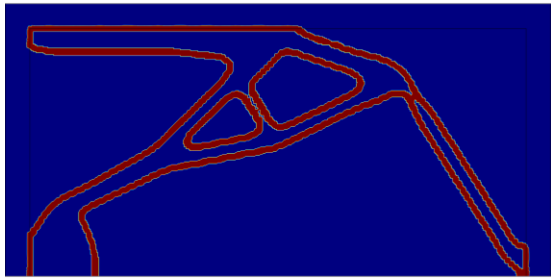

Macrostructure boundary density ρ_{bnd}

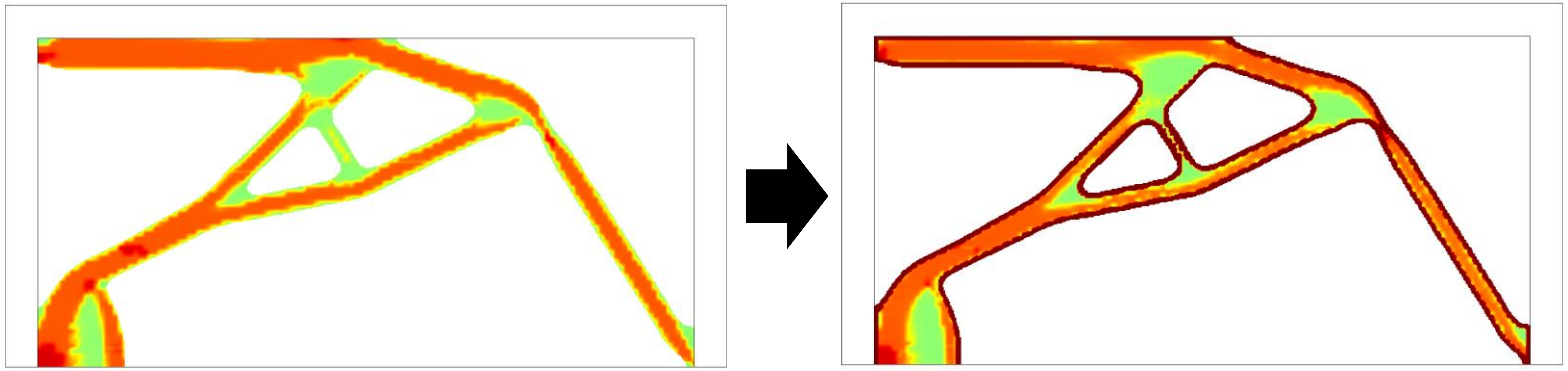

Infill density $(1-l_{y1})(1-l_{y2})$ before and after proposed post-processing

B. Design of infill microstructure

De-homogenization using explicit geometry (rotated rectangular)

- ✓ Explicit geometry representation imitating microstructure base cell
- ✓ Easy to handle small-sized microstructure unit cell
- ✓ Easy to generate mesh for re-analysis

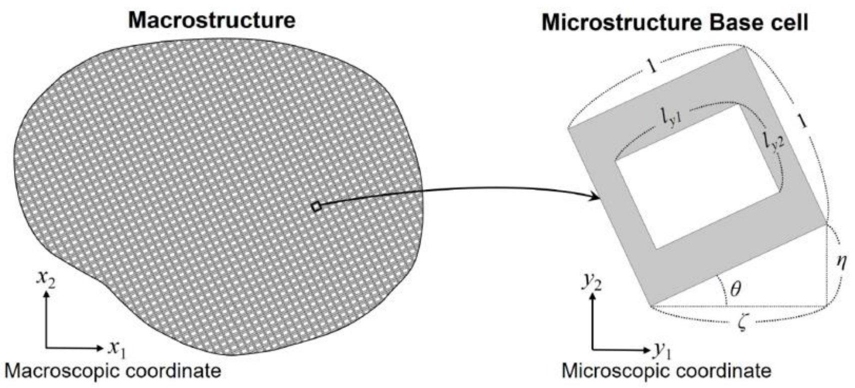

Microstructure with rectangular hole

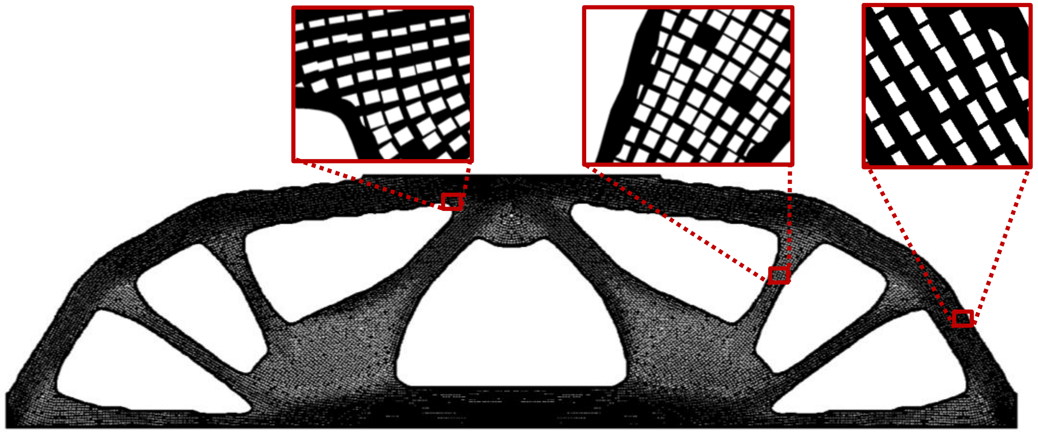

Infill structure with very small-sized microstructure unit cell

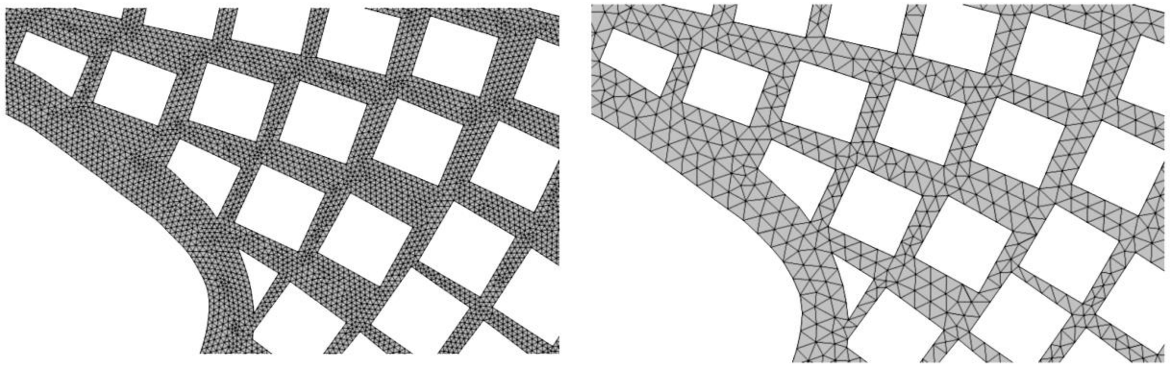

Finite element mesh for re-analysis of design result

Gwangju Institute of Science and Technology

B. Design of infill microstructure

De-homogenization using explicit geometry (rotated rectangular)

- ✓ From microstructure orientation fields $\boldsymbol{\zeta}, \boldsymbol{\eta}$, the density field $\boldsymbol{\rho}_{\mathbf{void}}$ representing square void region is obtained. Then, its centroid location is determined using image processing
- ✓ Rectangular voids are then removed from the macrostructure

$$\mathbf{e}_A(\mathbf{x}) = \begin{bmatrix} \zeta(\mathbf{x}) \\ \eta(\mathbf{x}) \end{bmatrix}, \quad \mathbf{e}_B(\mathbf{x}) = \begin{bmatrix} -\eta(\mathbf{x}) \\ \zeta(\mathbf{x}) \end{bmatrix} \qquad \mathbf{p}_i = \begin{bmatrix} \cos\left(2\pi\frac{i-1}{n_p}\right) \\ \sin\left(2\pi\frac{i-1}{n_p}\right) \end{bmatrix}$$

$$\nabla \cdot \left\{ (w_i^A(\mathbf{x}) + \epsilon_o)\left(\nabla \psi_i^A(\mathbf{x}) - \mathbf{e}_A(\mathbf{x})\right) \right\} = 0$$
$$\nabla \cdot \left\{ (w_i^B(\mathbf{x}) + \epsilon_o)\left(\nabla \psi_i^B(\mathbf{x}) - \mathbf{e}_B(\mathbf{x})\right) \right\} = 0$$

$$w_i^A(\mathbf{x}) = H\left(\rho(\mathbf{x}) - \frac{1}{2}\right) H\left(\mathbf{e}_A(\mathbf{x}) \cdot \mathbf{p}_i - \cos(\frac{2\pi}{n_p})\right) H\left(\mathbf{e}_A(\mathbf{x}) \cdot \mathbf{p}_{i+1} - \cos(\frac{2\pi}{n_p})\right)$$
$$w_i^B(\mathbf{x}) = H\left(\rho(\mathbf{x}) - \frac{1}{2}\right) H\left(\mathbf{e}_B(\mathbf{x}) \cdot \mathbf{p}_i - \cos(\frac{2\pi}{n_p})\right) H\left(\mathbf{e}_B(\mathbf{x}) \cdot \mathbf{p}_{i+1} - \cos(\frac{2\pi}{n_p})\right)$$

$$-R_w^2 \nabla^2 \begin{bmatrix} \tilde{w}_i^A \\ \tilde{w}_i^B \end{bmatrix} + \begin{bmatrix} \tilde{w}_i^A \\ \tilde{w}_i^B \end{bmatrix} = \begin{bmatrix} w_i^A \\ w_i^B \end{bmatrix}$$

$$w_i^{A_{bnd}}(\mathbf{x}) = H\left(\tilde{w}_i^A - 0.1\right) H\left(0.9 - \tilde{w}_i^A\right)$$
$$w_i^{B_{bnd}}(\mathbf{x}) = H\left(\tilde{w}_i^B - 0.1\right) H\left(0.9 - \tilde{w}_i^B\right)$$

$$w_i^{A_{ib}}(\mathbf{x}) = H\left(\tilde{w}_i^A - 0.1\right)$$
$$w_i^{B_{ib}}(\mathbf{x}) = H\left(\tilde{w}_i^B - 0.1\right).$$

$$\tilde{\rho}_m^A(\mathbf{x}) = H\Bigg(\sum_{i=1}^{n_p} \Big\{ \big[\tfrac{1}{2} + W_{tr}(P\psi_i^A(\mathbf{x}))\big] \big[w_i^{A_{ib}}(\mathbf{x}) - \tilde{w}_i^A(\mathbf{x})\big] W_{st}\Big(\mathrm{mod}\big(\sum_{j=1,\ j\neq i}^{n_p} [P\psi_j^A\ w_j^{A_{bnd}}] - P\psi_i^A\ w_i^{A_{bnd}}, 1\big)\Big) \Big\} \tilde{w}_i^A(\mathbf{x}) - \big[\tfrac{1}{2} + W_{tr}(1 - l_{y1}(\mathbf{x}))\big] \Bigg),$$

$$\tilde{\rho}_m^B(\mathbf{x}) = H\Bigg(\sum_{i=1}^{n_p} \Big\{ \big[\tfrac{1}{2} + W_{tr}(P\psi_i^B(\mathbf{x}))\big] \big[w_i^{B_{ib}}(\mathbf{x}) - \tilde{w}_i^B(\mathbf{x})\big] W_{st}\Big(\mathrm{mod}\big(\sum_{j=1,\ j\neq i}^{n_p} [P\psi_j^B\ w_j^{B_{bnd}}] - P\psi_i^B\ w_i^{B_{bnd}}, 1\big)\Big) \Big\} \tilde{w}_i^B(\mathbf{x}) - \big[\tfrac{1}{2} + W_{tr}(1 - l_{y2}(\mathbf{x}))\big] \Bigg).$$

$$\rho_{void}(\mathbf{x}) = \rho(\mathbf{x}) \tilde{\rho}_m^A(\mathbf{x}) \tilde{\rho}_m^B(\mathbf{x})$$

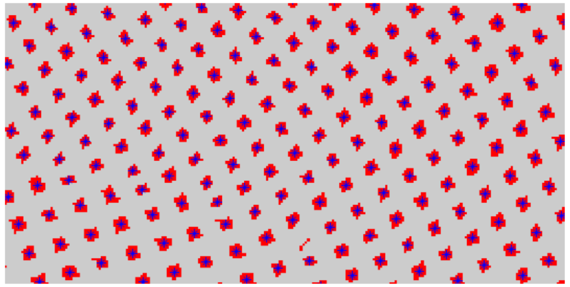

Centroid locations

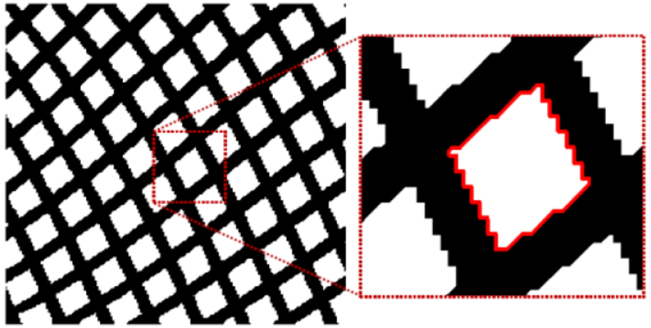

Infill design
using implicit density field

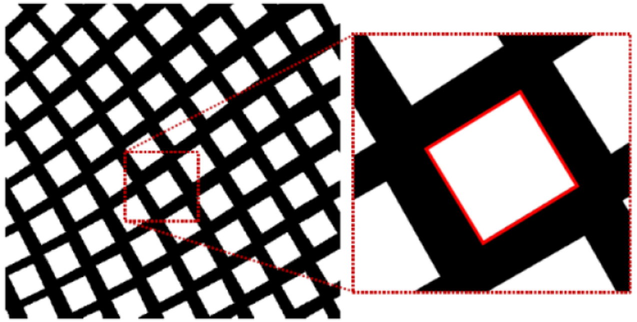

Infill design
using explicit rotated rectangular

Gwangju Institute of Science and Technology

Part 3
Numerical Examples

MBB Beam Design

Shell-infill design for compliance minimization problem

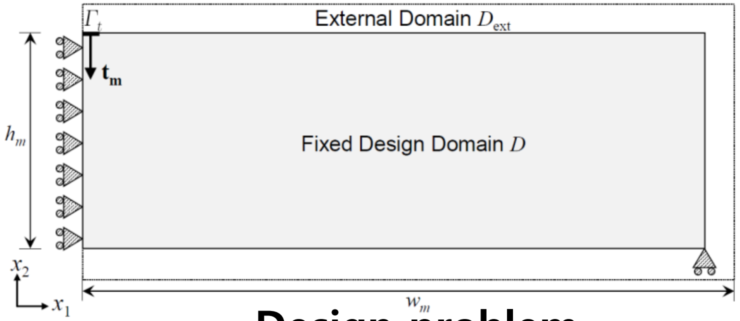

Design problem

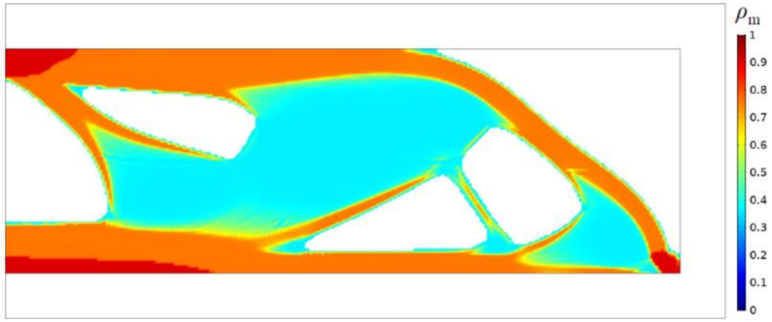

Microstructure density field ρ_m

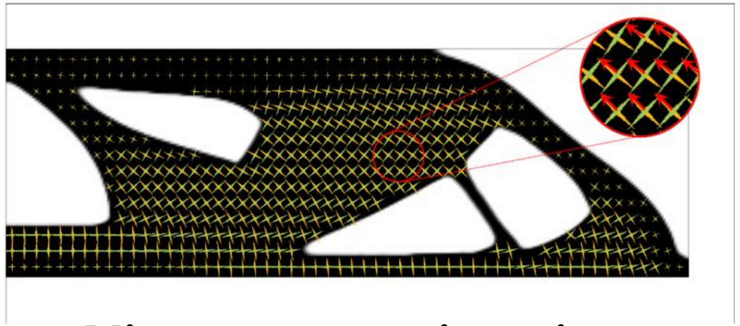

Microstructure orientation

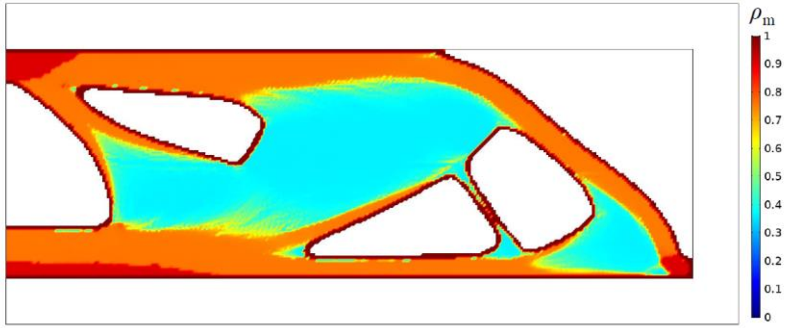

Coated structure after post-processing

Compliance value (Φ)	Volume fraction (V/V_{tot})
233.90	0.3988

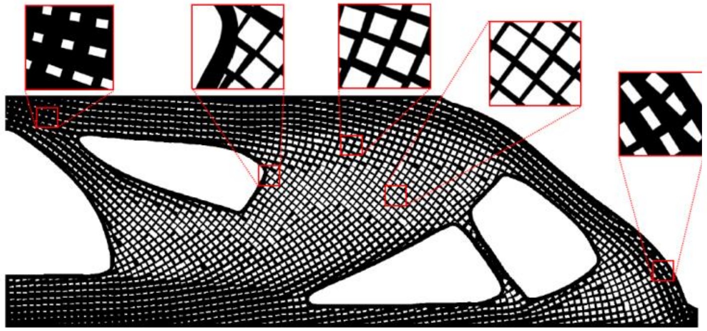

Restored infill structure

Compliance value (Φ)	Volume fraction (V/V_{tot})
232.64	0.4004

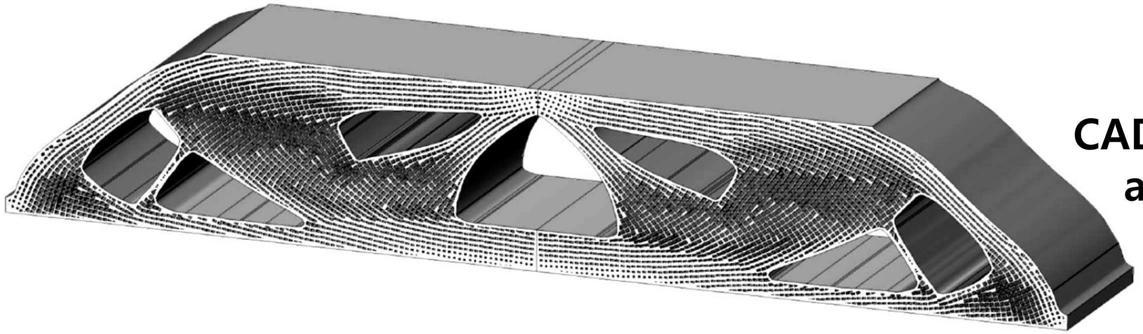

CAD model for additive manufacturing

Gwangju Institute of Science and Technology

MBB Beam Design

Shell-infill design for compliance minimization problem

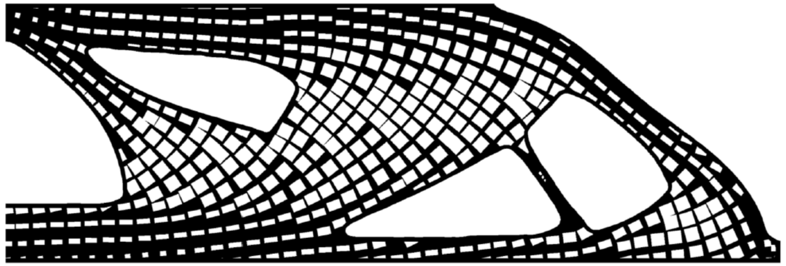

Number of cell per unit length P=15

Compliance value (Φ) 244.64

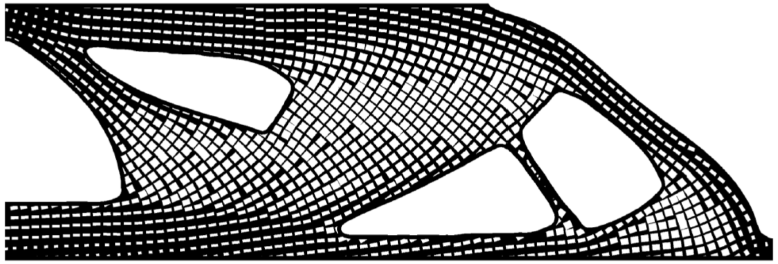

Number of cell per unit length P=25

Compliance value (Φ) 238.81

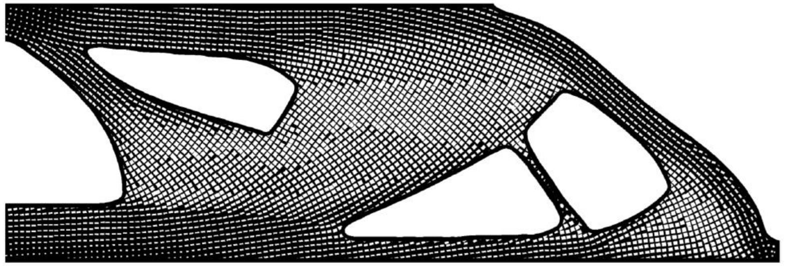

Number of cell per unit length P=45

Compliance value (Φ) 231.87

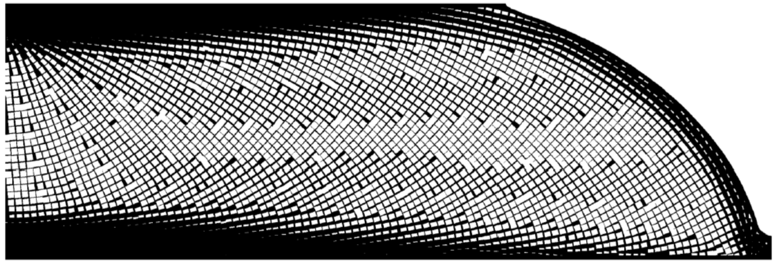

$l_{lower}=0$, $l_{upper}=0.9$

Compliance value (Φ) 194.73

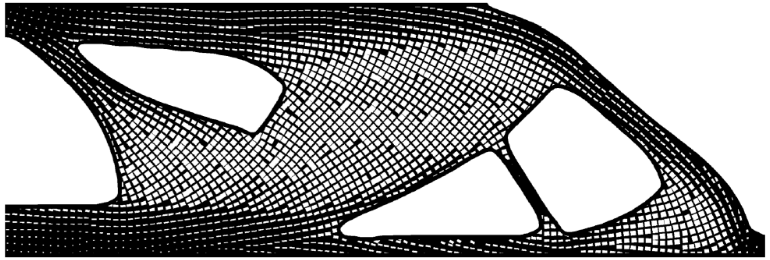

$l_{lower}=0.2$, $l_{upper}=0.8$

Compliance value (Φ) 224.60

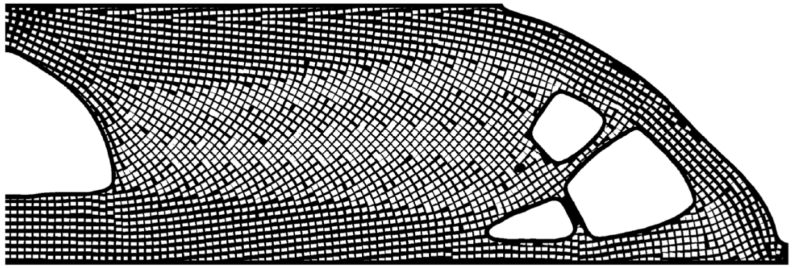

$l_{lower}=0.5$, $l_{upper}=0.8$

Compliance value (Φ) 263.91

Bell Crank Design

Shell-infill design for compliance minimization problem

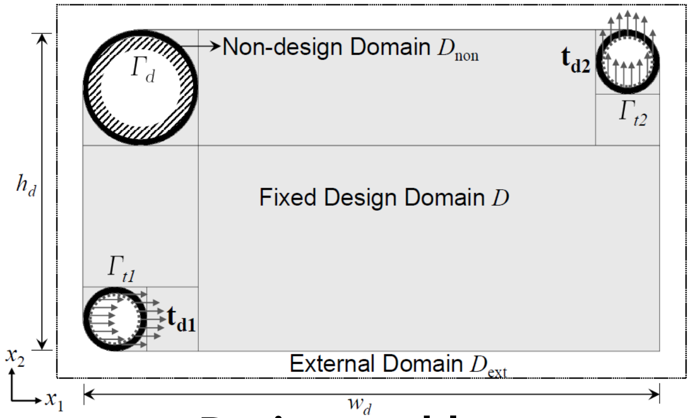

Design problem

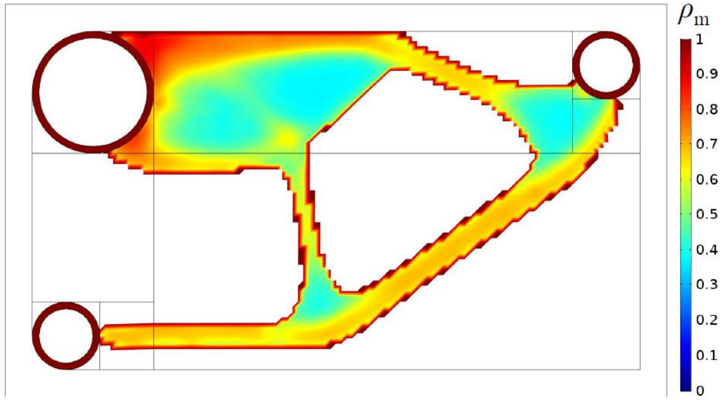

Microstructure density field ρ_m

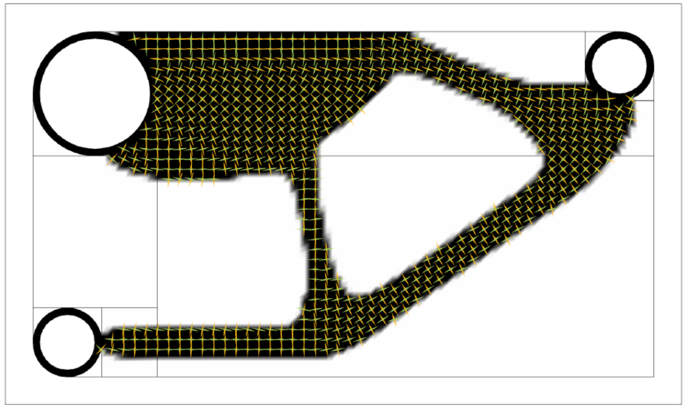

Microstructure orientation

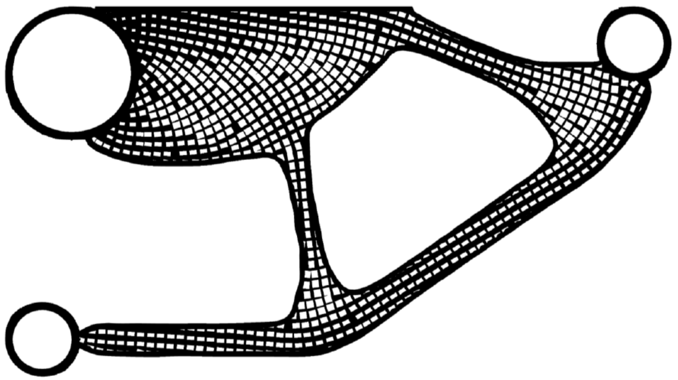

Design result with restored infill structure

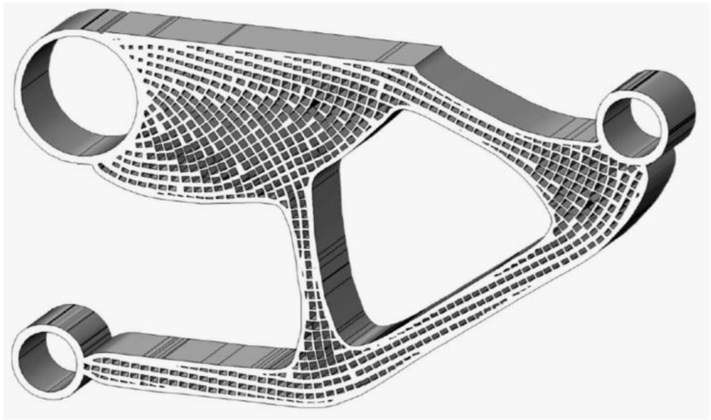

CAD model for additive manufacturing

Bell Crank Design

Shell-infill design for compliance minimization problem

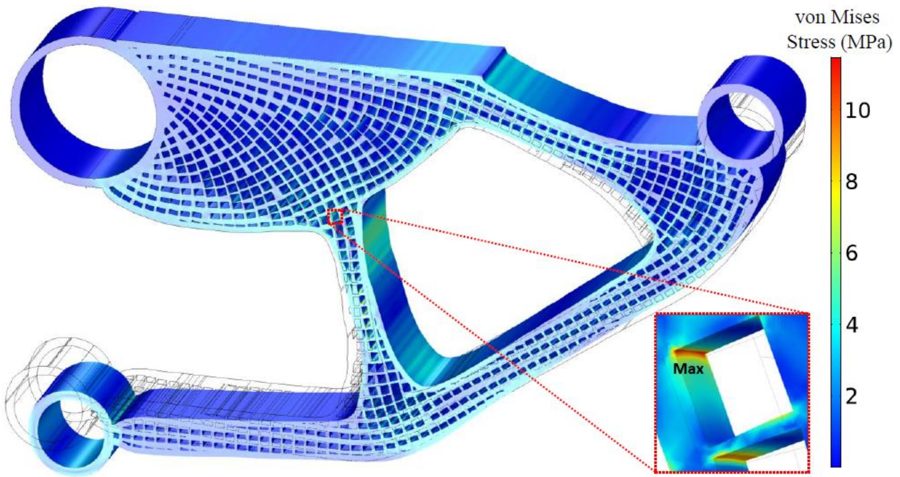

CAD model and its reanalysis result

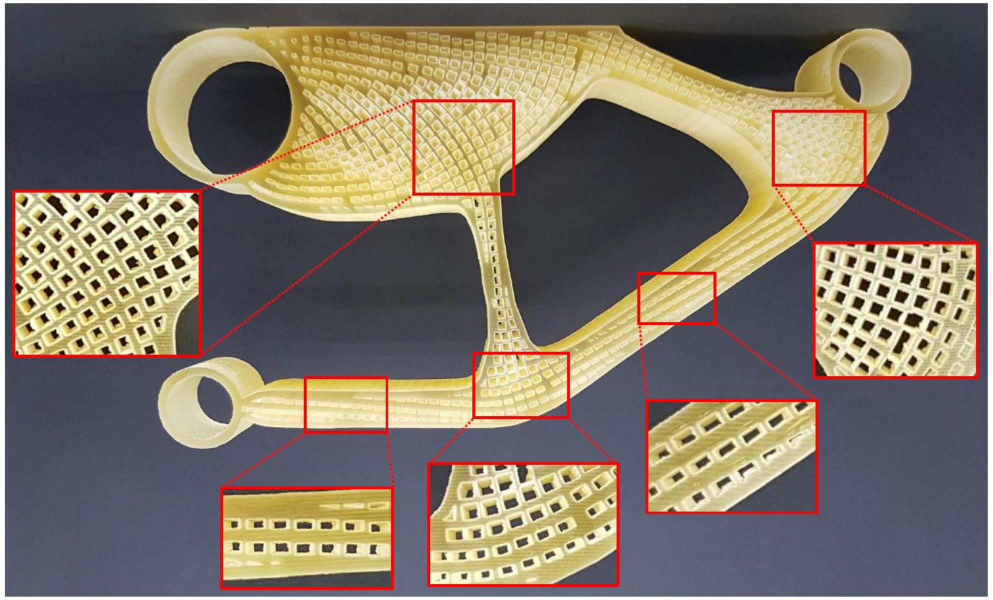

Additive manufactured design result

Size: 240 X 150 X 30 mm

Model: A multi-jet printing machine (Projet 3510 SD)

Resolution: 0.0250-0.05 mm per 25.4mm

Printing material: Ultraviolet curing plastic (Visijet M3 Crystal)

Bell CrankDesign

Shell-infill design for compliance minimization problem

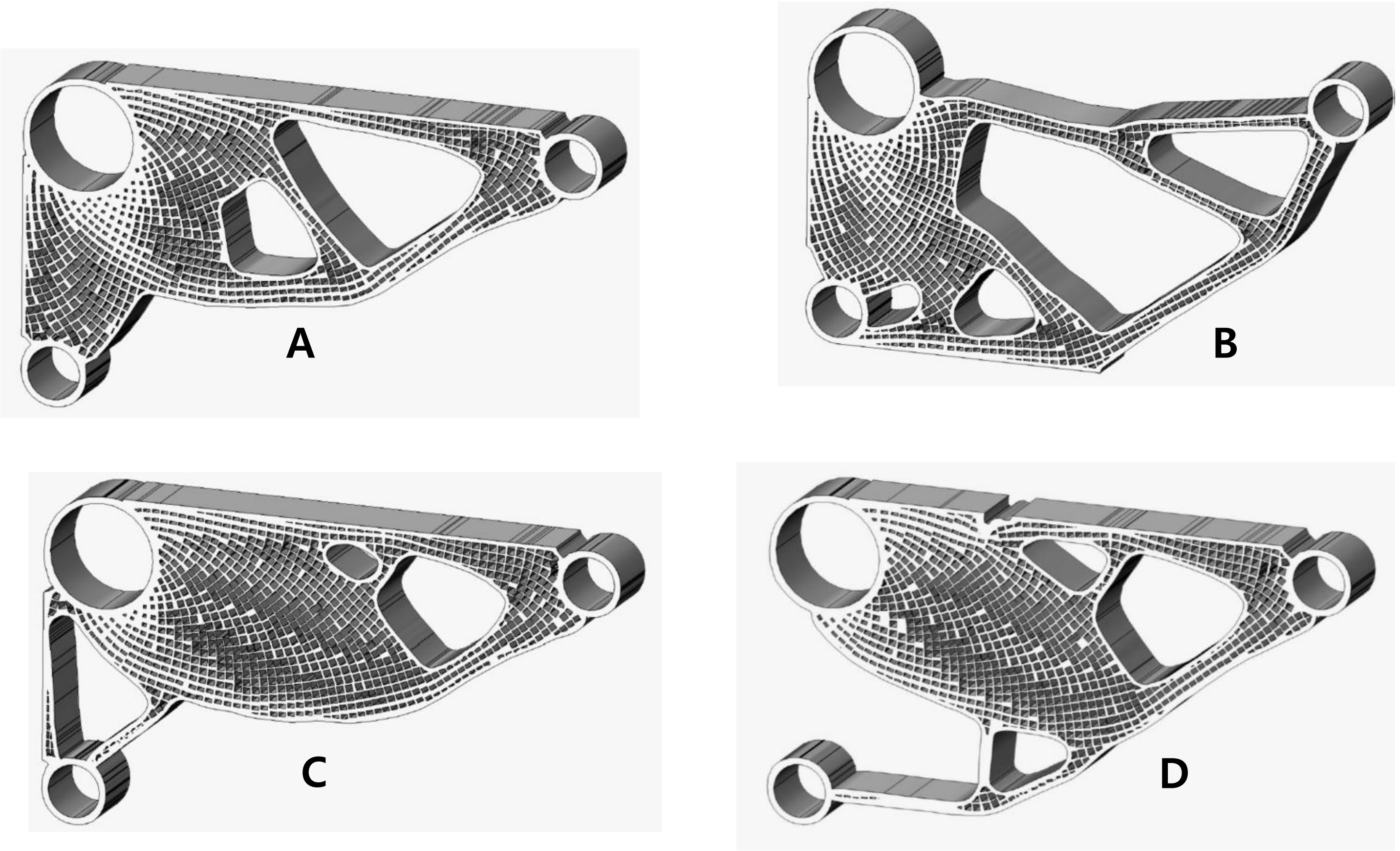

Design result with various loading conditions

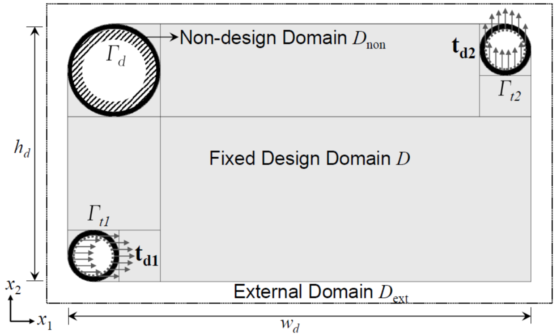

	$\mathbf{t_{d1}}$ (traction at Γ_{t1})	$\mathbf{t_{d1}}$ (traction at Γ_{t2})
A	$(1,0)\ N/m^2$	$(0,1)\ N/m^2$
B	$(-\frac{5}{3},0)\ N/m^2$	$(0,\frac{1}{3})\ N/m^2$
C	$(\frac{1}{3},0)\ N/m^2$	$(0,\frac{5}{3})\ N/m^2$
D	$(-\frac{1}{3},0)\ N/m^2$	$(0,\frac{5}{3})\ N/m^2$

loading conditions

Any Questions?